Enhanced separation of aged RBCs by designing channel cross section

Yuanyuan Chen,[1] Yuzhen Feng,[2] Jiandi Wan,[3] and Haosheng Chen[1,a)]
[1]*State Key Laboratory of Tribology, Tsinghua University, Beijing 100084, China*
[2]*School of Mechanical Engineering, University of Science and Technology Beijing, Beijing 100083, China*
[3]*Department of Microsystem Engineering, Rochester Institute of Technology, Rochester, New York 14623-5608, USA*

(Received 2 February 2018; accepted 2 March 2018; published online 13 March 2018)

Prolonged storage will alter the biophysical properties of red blood cells (RBCs), and it decreases the quality of stored blood for blood transfusion. It has been known that less deformable aged RBCs can be separated by margination, but the recognition of the storage time from the separation efficiency of the stiff RBCs is still a challenge. In this study, we realized enhanced separation of aged RBCs from normal RBCs by controlling the channel cross section and demonstrated that the storage time can be deduced from the percentage of the separated RBCs in the stored RBCs. This separation technology helps to reveal the regulation of time on the RBC aging mechanism and offer a new method to separate stiffened cells with high efficiency. *Published by AIP Publishing*. https://doi.org/10.1063/1.5024598

I. INTRODUCTION

Red blood cells (RBCs) undertake the function of delivering oxygen to the body tissues, and the deformability of RBCs enables them to get through small capillaries.[1] The deformability of RBCs can be altered naturally by various pathophysiological conditions, including malaria,[2] sickle cell disease,[3] diabetes,[4] and sepsis,[5] and artificially by chemicals.[6–8] RBCs will lose deformability with growing age when they circulate in venules,[9] until hemolysis or cleaned by spleen. Recently, the deformability of stored RBCs raises much concern for safe blood transfusion.[10,11] Transfusion with high-quality is essential to modern health care;[12] however, known as the "storage lesion,"[13–15] complex biochemical and physiological changes caused in the storage process increase the transfusion risks. A significant loss of deformability will happen after the RBCs are stored above 14 days, and the loss is not reversible.[11] The aged RBCs after storage will be harmful to the blood transfusion, with the increasing risk of RBC retention, thrombosis, and haemolysis.[16] Moreover, the extracted blood contains RBCs with different ages, and the old RBCs will lose most of their deformability and have extreme high stiffness in the same storage time. These aged RBCs would be especially harmful to the blood transfusion. Recent microfluidic work on RBCs also emphasized the effect of RBC deformability in health and disease.[17–19] Therefore, it is necessary to know the dependence of deformability on the storage time and separate the aged RBCs from the blood for safer blood transfusion.

Margination is originally used to describe the migration of leukocytes and platelets to the vessel wall in blood vessels, and the margination mechanism has been revealed in many ways.[20–23] Size, shape, and deformability affect the margination performance of objects in shear flow, and the margination theory has been applied to the study of cell sorting technology and drug delivery *in vivo* and *in vitro*. As a viscoelastic fluid, blood in vessels offers the first normal stress for rigid objects to perform margination. Under the effect of the first normal stress, RBCs will approach the wall in a shear flow, and the interaction between a soft membrane and

a)Author to whom correspondence should be addressed: chenhs@mails.tsinghua.edu.cn

the wall generates a high lift force that will pushes the cell away from the wall.[20] However, a rigid RBC lacks such a high lift force to push it away from the wall, resulting in the separation from soft RBCs and the realization of margination. As a rigid particle, drug delivery processes in blood are also largely dependent on margination theory.[23] As a new technology, microfluidic devices offered a fast and simple method for cell sorting with high efficiency and low cost. Recently, the separation of stiffened cells (SCs) has been realized in microfluidic devices based on the margination theory. It has been used to separate diseased RBCs for better diagnosis and therapy, for instance, the purification of malaria-infected RBCs and sepsis-infected RBCs from normal RBCs.[24,25] The stiffened RBCs would perform lateral motions toward the channel wall under the first normal stress generated in the viscoelastic RBC suspension or polymer solution.[24] Also, the deformability-based cell sorting method was applied to enrich less deformable RBCs from stored blood.[26] Yet, the sorting efficiency is not high enough for the next commercial application, and it is still unclear that whether the storage time affects the separation efficiency (SE). It inspires us to study the enhanced separation of aged RBCs and the recognition of the storage time from the separation efficiency of aged RBCs.

In this paper, particle performances in different viscoelastic fluids were first investigated to find the best flow condition for the separation of aged RBCs. Microchannels with different cross section shapes were then designed to obtain the enhanced separation efficiency. It should be noted here that a traditional rectangular microchannel is compared to a new designed triangular microchannel on the separation efficiency, and the triangular channel is demonstrated to be a better one to separate and detect aged RBCs. Furthermore, RBC performances in the triangular microchannel were compared to investigate the relationship between storage time and separation efficiency, and the mechanism was clarified by analyzing the RBCs' modulus changing pattern over storage time. This research may not only help to understand the metabolism of RBCs during their span life but also bring us a new insight into the cell separation technology to reduce the risk in blood transfusion.

II. METHODS

A. Microfluidic device

Devices with a triangular cross section were fabricated using a metal mode, as shown in Fig. 1(a). The cross section shape was controlled through mechanical processing to an isosceles triangle with a bottom angel of 30°, and the base length is 100 μm. The liquid polydimethylsiloxane (PDMS) was poured on the mode, and after air exhausting, the mode with PDMS was put on the hot plate with a temperature of 150 °C for baking. 5 min later, and the PDMS channel was solidified and removed from the metal mode. This PDMS mode was then bonded with a PDMS slide with a height less than 1 mm using a plasma gun (BD-20ACV, Electro-Technic). After 30 min baking at the temperature of 100 °C, the microchannel with a triangular cross section was fabricated. Devices with a rectangular cross section were fabricated using the standard polydimethylsiloxane (PDMS) lithographic method.[27] The structure of the microfluidic device is shown in Fig. 1(b). The height of the microchannel used in Fig. 2 is 10 μm and in Fig. 3 is 25 μm. The microchannel has 3 sections. The first section is the inlet with a converge shape. The second section is a straight microchannel with the widths of 45 μm for Fig. 2 and 100 μm for Fig. 3. The third section has a diverge shape, and it is the outlet of the constriction channel. The top views at these three sections show the margination process of particles in the rectangular channel, and the cross sectional views [inset pictures (i) and (ii)] show the effect of margination on particles' distribution in different sections of the channel. Moreover, there are three reservoirs at the outlet of the device, distributed in the side and center of the channel to collect the separated RBC suspensions. The separated particles were observed at this section, as the inset picture (iii) shown in Fig. 1(b). Before use, all the channels were pumped into phosphate-buffered saline (PBS) solution with 2.5 g/l bull serum albumin (BSA) to prevent cell adhesion. The mean flow rate was controlled as 1 mm/s in all flowing experiments.

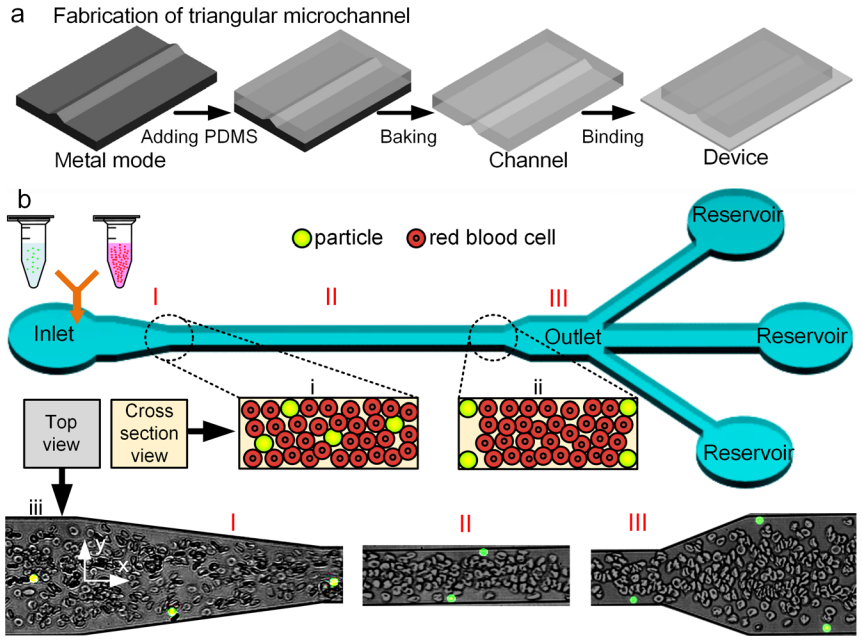

FIG. 1. The schematics of the microfluidic device for the margination experiment. (a) The fabrication process of the triangular microchannel. (b) The structure of the rectangular channel; the inset figures of (i) and (ii) illustrate the distribution of the particles in different sections of the channel and (iii) shows the observed margination of the particles at three sections of the microchannel with red blood cells.

B. Particle sample

Fluorescent particles (polystyrene-based, 7%v/v, Excitation max = 441 nm, and Emission max = 486 nm, Polysciences, Inc.) with the diameter of 6 μm were mixed with PBS buffer, polyethylene oxide (PEO) solution, and the RBC solution, at the concentration of 0.03%v/v, resulting in a ratio of RBCs (30%Hct) to particles in the sample of 1000 (30%/0.03%), which matches the ratio of RBCs to leukocytes in the blood. The shear modulus of the particles is 700–800 MPa, and the size of the particle is chosen to match the size of RBCs to obtain cell sorting conditions for cell margination without the size difference effect.[28]

C. PEO solutions

PEO is a commonly used polymer to enhance the viscoelasticity of fluid in the study of particle margination, and its viscoelasticity has been well analyzed in previous research.[28,29] Polyethylene oxide (PEO, Mw = 4 000 000, Sigma Aldrich) was suspended in phosphate-buffered saline (PBS, 1X without Ca^{2+} and Mg^{2+}, Hyclone) buffer with the concentration of 0.2%wt to achieve the PEO solution.

D. RBC solutions

The blood used in this experiment was taken from healthy adults, washed with PBS buffer, and then subjected to centrifugation (Eppendorf AG) at 3000 r/min for 75 s each time, and the centrifugation was repeated 3 times to get the packed RBCs. The packed RBCs were re-suspended in PBS buffer to achieve the RBC solution with the corresponding hematocrit (Hct) for the next experiment, and 30%Hct was used for Fig. 2.

E. Aged RBC sample

After washing, the leukocytes and platelets are removed from the freshly taken blood. Then, the main part of the packed RBCs is re-suspended in PBS buffer to compose the RBC

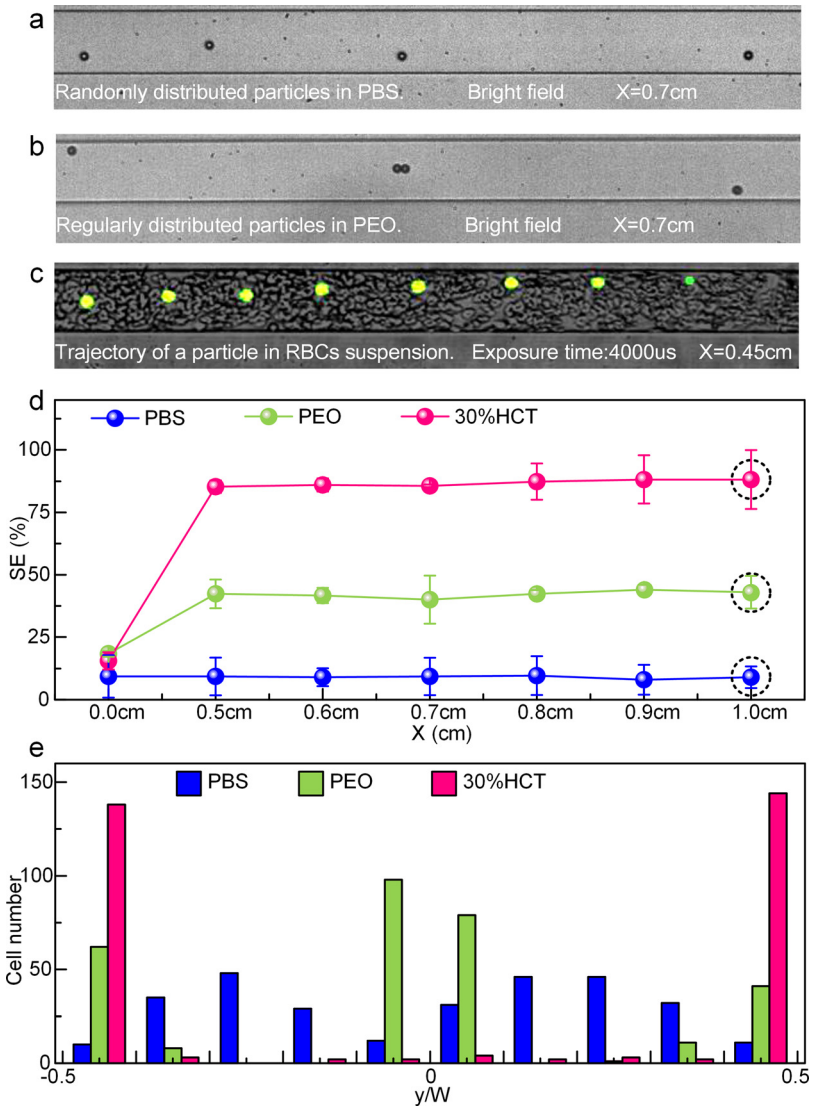

FIG. 2. Margination of particles in RBC, PEO, and PBS solution. (a) Random distribution of particles flowing in PBS solution. (b) Particle motion in PEO solution with three equilibrium positions. (c) Migration trajectory of a particle in RBC solution, and the picture shows the superposition of the fluorescent particles under the fluorescent field with the bright field, and the trajectory of the particles is from the different positions of one particle at different moments, as described in method "G." (d) Separation efficiency of particles flowing in different solutions along the channel length. The dashed circles represent the observation conditions in (e). (e) Lateral distribution of particles across the channel at the length of 1 cm in the 3 kinds of solutions.

solution in point "D," and the other part of the packed RBCs is suspended in PBS with 1 mg/ml bull serum albumin (BSA, Sigma) and then stored in a refrigerator at 3–4 °C to prepare the aged RBC sample. The freshly taken RBCs are the 0 day RBCs, and it is also called normal RBCs in this paper. 1 day RBCs means that the storage time is 24 h. Before use, the stored RBC suspension will be washed again using PBS buffer to get the target aged RBCs, and the washing protocol is the same to point "D." In order to distinguish the target RBCs from normal RBCs during their flowing in the microchannel, before mixing with normal RBC solution, the target RBCs were stained by 1 mg/ml fluorescein isothiocyanate isomer I (Sigma-Aldrich) suspending in PBS buffer. After 3 h incubation in a water bash at 37 °C, the target RBCs were re-washed using PBS buffer, and then, they were added into the RBC solution at the concentration of 0.03%v/v to achieve the aged RBC sample for the sorting experiment.

F. Modulus test process

The Young's modulus of RBCs was measured to investigate the revolution of RBC stiffness on storage time. As described in a previous study, a standard biological Nanoindenter (Piuma, Optics11, Probe stiffness: 0.46 N/m, Tip radius:52.5 μm)[30] was applied to this study. Applying the Hertzian model to describe the indentation of elastic RBCs,[31] the Nanoindenter uses a loading section of the load-displacement curve to determine the Young's modulus of RBCs during testing. Allowing for the depth of RBCs, a fit of all data points from the contact point to 5% of the maximum load point is chosen to obtain the Young's modulus. This ratio was set in the testing software before testing, and after the test, you will get an automatic fitting modulus value. For experiments, the Piuma Nanoindenter is placed on the top of a regular lab bench, and the testing is automatically performed through the specific software control. As for the testing target, RBCs with different storage times (from 0 day to 29 days) were mixed with PBS buffer at the concentration of 0.2%v/v, and the concentration was chosen to ensure the effect of cell adhesion on the glass slide in the next step. Then, the solutions were placed on the glass slide coated by Poly-L-Lysine (LIUSHENG). After 10 min, the glass slides were washed with the PBS buffer, while the cells were kept on the glass slide. PBS buffer was added again on the glass slide to support RBCs, and then, the prepared glass slide with the adhered RBCs was placed on the bottom of the indenter. After the indenter merged into the droplet of PBS, more PBS buffer was added to confirm that the measurement could be finished with the indenter and RBCs fully merged in PBS buffer.

G. Experiment procedures and image analysis

The motions of the flowing particles/RBCs in the channel were captured using the fast camera (M710, Phantom Co.) under the fluorescent field provided by an inverted microscope (LEICA DME6000 B), while the background was captured in the bright field at the same position. The frame rate was set as 24 fps to get the biggest exposure time of 41 000 μs of the camera, and under this exposure time, the flowing of fluorescent target RBCs could be clearly captured. First of all, the fast camera was connected to the microscope to replace the microscopy's original CCD. Switching the microscopy lens to $\times$20 and regulating the focal length and the observation platform to find the channel, the flow of particles and RBCs could be observed from the camera's software. The parameters of the camera to achieve clear flowing of particles and RBCs in the microchannel are regulated. The motions of particles in PBS buffer and PEO solution were captured under the bright field, and the motions of particles and target RBCs in RBC solution were captured under both the bright field and the fluorescent field. After the shooting, the obtained videos were analyzed through Image J. Specifically, the trajectory of the particle in RBC solution was extracted from a video of particle flowing in RBC solution. The images of the particle in RBC solution at different frames were output from Image J first, and then, the images were montaged by using Photoshop software to exhibit the trajectory of particle flowing in RBC solution. In order to show the relative position of the particle to RBCs, the background captured in the bright field at the same position was added at the back of the fluorescent image, and the transparency of the fluorescent image was regulated to clearly show the bright image. The final impression drawing is shown in Fig. 2(c). As for the sorting efficiency and particle distribution, we marked a position on the channel when playing the video in Image J, and therefore, we could count the target particles and RBCs at the same position. The distance of target particles and RBCs to the channel wall was measured through Image J, and the measuring results were saved into an Excel file. Then, the data were input into the Origin to obtain the particle distribution. At last, the figures are plotted in Origin.

H. Fluorescent dot observation from the reservoir

The reservoir was fabricated by a hole puncher with a diameter of 4 mm before the channel was bonding on a PDMS slide. 30 μl PBS buffer was pre-added in the reservoirs before the

experiment. After the experiment, the separated RBC suspension collected at the reservoir was taken out using the pipette and put on a glass slide to conduct the fluorescent dot observations.

III. RESULTS

A. Margination of particles in the RBC suspension

To find the best separation condition, the performance of solid particles in PBS, PEO, and RBC solutions was first investigated. The fluorescent particles were mixed with three solutions, respectively, and they were pumped into the microchannel using a syringe pump. The particles suspended in the PBS solution and PEO solution were used as the control groups. It is found that particles in PBS solution are randomly distributed across the channel, and the margination does not happen, as shown in Fig. 2(a). The margination of particles happens in the PEO solution, and the particles have three equilibrium positions in the channel, the wall on the both sides and the center of the channel, as shown in Fig. 2(b). This result is consistent with the previous studies that stiffen particles will perform margination in viscoelastic fluid.[24,25] The rectangular channel width (W) and height (H) are 45 μm and 10 μm, respectively. Allowing for the definition of hydraulic diameter $D_w = 2WH/(W+H)$ and the blockage ratio $\kappa = a/D_w = 0.37 > 0.25$, under this flow condition, normal stresses push the particles toward the wall.[28,32] However, the center equilibrium position does not appear for the particles flowing in the RBC solution, as shown in Fig. 1(c). It is considered that the particles staying in the center would be pushed aside by the interactions with RBCs and perform the margination to the channel wall.

The locations of particles and cells along the channel width at different channel lengths were counted and represented by the separation efficiency (SE), which is defined as $SE = N_{wall}/N_{total}$, where N_{wall} is the number of the particles flowing close the channel wall with the distance less than 4.5 μm (1/10 W; W is the channel width and represented by "y," and this area is also defined as the margination zone), and N_{total} is 100 observed particles at the same observation. The SE provides a quantitative result on the margination of particles in the three kinds of solutions. It is obviously higher in RBC solution than that in PEO solution, while there is no margination effect in PBS solution, as shown in Fig. 1(d). The particle's lateral distribution across the channel at the length of 1 cm [the dashed circle in Fig. 1(d)] was measured and is plotted in Fig. 1(e). The particles have 3 equilibrium positions in PEO solution and 2 equilibrium positions in RBC solution, while they present homogeneous distribution in PBS solution.

This study has demonstrated that the viscoelasticity of solution could trigger the margination of particles in the rectangular microchannel, and the collisions between the RBCs and the particles during flowing would push the particles away from the center equilibrium position, resulting in the disappearance of the center equilibrium positions of particles in RBC solution. Therefore, more stiff particles would migrate to the side wall of the channel when they flows in the RBC suspension. Accordingly, the RBC suspension has the priority to realize cell sorting with higher separation efficiency than viscoelastic PEO solution.

B. Cell separation in rectangular and triangular microchannels

According to the margination experiment for particles shown in Fig. 2, the channel length of 1 cm is enough for the RBCs to migrate to the wall in a 100 μm × 25 μm rectangular channel. Allowing for the consumption of blood during the detection, the RBC suspension with 20%Hct is used in this experiment. RBCs with storage times of 0 day, 6 days, 18 days, 24 days, and 29 days were prepared and fluorescently dyed as the target cells.

Since the first normal stress could be expressed as $F_N \sim \mu\lambda\nabla\dot{\gamma}^2$,[33] the direction of the normal stress is the same as the gradient of the shear rate, $\nabla\dot{\gamma}$, and the gradient of the shear rate on the cross section of the microchannel could be obtained through Comsol Multiphysics. Figure 3(a) shows the first normal stress distribution on the rectangular cross section, and the low stress zone (blue color) predicts the equilibrium positions of stiffened RBCs in the microchannel. The RBC performance in the microchannel under bright and fluorescent fields is shown in Fig. 3(b). SE was calculated to clarify the separation of aged RBCs. Following the

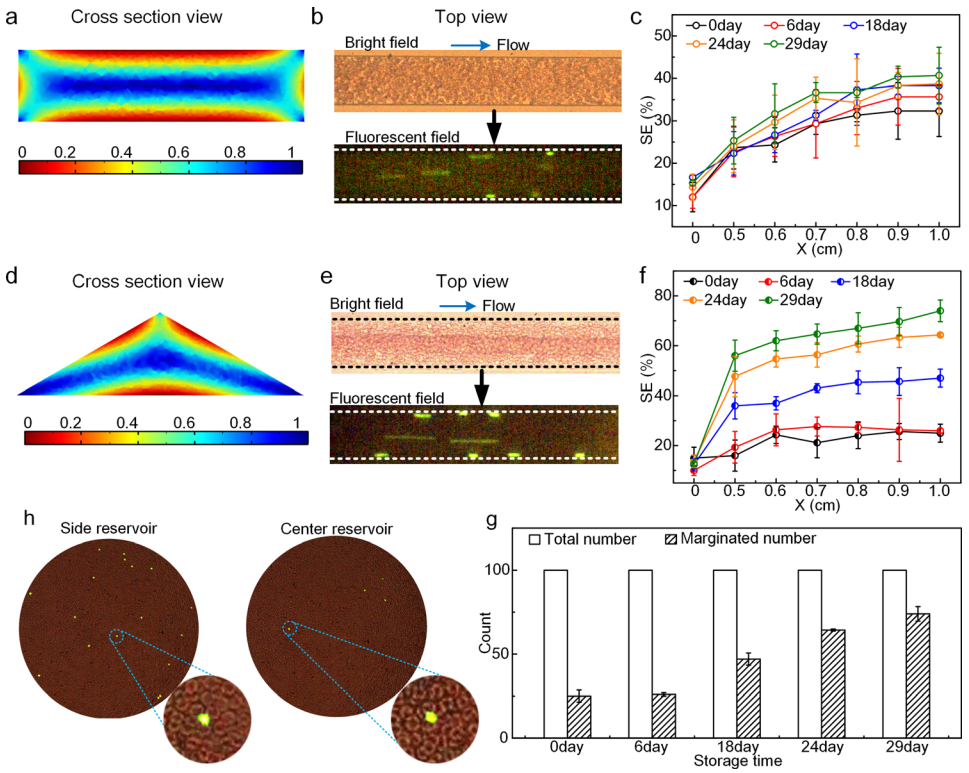

FIG. 3. Margination of aged RBCs in rectangular and triangular channels. (a) The first normal stress distribution on the rectangular channel cross section, and the color represents the relative magnitude of the first normal stress. (b) The performance of aged RBCs in the rectangular channel under bright and fluorescent fields. The dashed lines represent the channel edges, the bright dots represent the fluorescent 29 day RBCs, and the figures were captured at 1 cm of the channel. (c) The variation of SE of aged RBCs with different storage times in the rectangular channel. (d) The first normal stress distribution on the triangular channel cross section. (e) The performance of aged RBCs in the triangular channel under bright and fluorescent fields. (f) The variation of SE of aged RBCs with different storage times in the triangular channel. (g) Cell number alternation of marginated RBCs along storage time at the position of 1 cm of the triangular channel. (h) The fluorescent dot observation of 29 day RBCs from side and center reservoirs. The dashed circles represent the partial enlarged views.

counting rules in Fig. 2, 100 cells were counted in every point in Fig. 3(c), and each point was repeated three times in the experiment. It is obvious that the SE increases along the channel length, and the 29 day RBCs have the highest SE. However, the SE is so low that could not be used as a separation method to sort RBCs. Moreover, the difference between the SE of each sample is dedicate and not enough to be used as a bio-mark to detect aged RBCs. Actually, our previous study has demonstrated that the cross section shape of the microchannel could affect the margination of RBCs in viscoelastic solution, and an acute angle could result in a high separation efficiency.[34] Therefore, the triangular microchannel was applied in this experiment. As shown in Fig. 3(d), the first normal stress distribution is over the triangular cross section, and the flow rate was controlled as the same with that in the rectangular microchannel. This distribution shows a bigger margination zone (blue color) near the channel wall in the triangular channel than that in the rectangular channel. Under the same flow condition, the RBC performance in the triangular microchannel under bright and fluorescent fields is shown in Fig. 3(e), and the SE variations of target RBC samples along the channel length are shown in Fig. 3(f). Obviously, the SE in the triangular channel is enhanced comparing with that in the rectangular channel. In addition, the aged RBCs performed visible distinction over storage time in the triangular microchannel between 6 day, 18 day, 24 day, and 29 day. While the SE of 0 day and 6 day RBCs are similar, it is considered that 6 days is not enough for RBCs to perform a significant change on deformability and behave like stiff cells. Furthermore, at the same position along the length of the microchannel, the RBCs with longer storage time have higher sorting efficiency. That is, at this location, RBCs with different storage times distribute at the distinct

position along the channel width, from the channel wall to the channel center, the storage time of the distributed RBCs is from long to short, and the age of the distributed RBCs along the channel width is in a descending order. Allowing for the high SE and the visible distinction between aged RBCs, the SE of aged RBCs from normal RBCs could be enhanced by controlling the channel cross section shape, and the triangular channel has the priority to be used as the cell separation channel for the elimination of aged RBCs.

To clarify the relationship between SE and storage time for cell detection, the marginated cells at the position of 1 cm of the triangular channel were counted in every 100 observed cells, and the results from 300 cells are shown in Fig. 3(g). The marginated cell is defined as the cell flowing in the margination zone. It should be noted that some RBCs are also separated from 0 day blood, and it can be understood because blood may contain some old RBCs with high modulus. Some target cells might already stay in the margination zone when they entranced the channel. The number of marginated cells increases from 25 ± 3 to 74 ± 4 per 100 as the storage time is elongated from 0 day to 29 days. That is, RBCs with different storage times perform a distinct level of margination, and as the storage time increased, more and more RBCs entranced into the margination zone when they were flowing in the triangular microchannel.

On the other hand, SE could describe the probability of aged RBCs' margination happening in the microchannel, and allowing for the visible distinction between aged RBCs with different storage times, the SE in the triangular channel could be used as a bio-mark to detect the storage time of blood. However, SE is a dynamic counting value, and it is hard to be used allowing for the detection application. Therefore, the fluorescent dot observation at the outlet of the separation device was performed to prove the utility of this detecting method. 29 day RBCs were prepared and mixed with normal RBCs, and under the same flow condition as shown in Fig. 3(e), the separated RBCs were collected at the outlet reservoirs of the device with the triangular microchannel. The fluorescent cells separated in the side reservoir were compared to those unseparated in the center reservoir. As shown in Fig. 3(h), the bright dots are the stained 29 day RBCs, and the picture was obtained under the fluorescent field, and the background was obtained under the bright field at the same position. It is obvious that the separation of 29 day RBCs from normal RBCs was realized. Furthermore, 251 target cells from 10 obtained pictures were counted, and the ratio of target cells from the side is 80.88%, which is a little higher than the results in Fig. 3(f). It can be understood that we counted the target cells flowing in the margination zone in Fig. 3(f), which is strict. However, during the observation in Fig. 3(h), some targets cells that were close to the margination zone might entrance into the side collecting reservoir, which increased the ratio in Fig. 3(h). This result verified our margination theory on detecting aged RBCs and showed its potential application in recognition of the aged RBCs with high efficiency.

C. Dependence of SE on RBC modulus

It has been knowing that the storage process would cause the deformability loss of RBCs, and the aged RBCs could be separated from normal RBCs based on margination.[16,26] However, in the above study, we have demonstrated that RBCs with different storage times performed different levels of margination, resulting in distinct SE. That is, the recognition of storage time from separation efficiency of aged RBCs is realized, while the mechanism between them is still unclear. If we define the process of RBCs' deformability loss as the stiffened process by storage time, it is hypothesized that the stiffened rate of storage time on RBCs regulates the margination of aged RBCs in the microchannel. As described in method "F," the Young's modulus of RBCs was measured to investigate the dependence of SE on RBC stiffness. RBCs with storage times of 6 days, 18 days, 24 days, and 29 days were prepared, and the RBCs without storage (0 day) were used as the control group. For each kind of aged RBCs, their modulus was measured 3 times, and 40 cells were measured in each time.

The RBCs in different storage times express different Young's modulus distributions, as shown in Fig. 4(a). As the storage time increased, more RBCs became stiffer. We defined the area with modulus higher than or equal to the maximum of 0 day modulus (E_{0max}) which is the

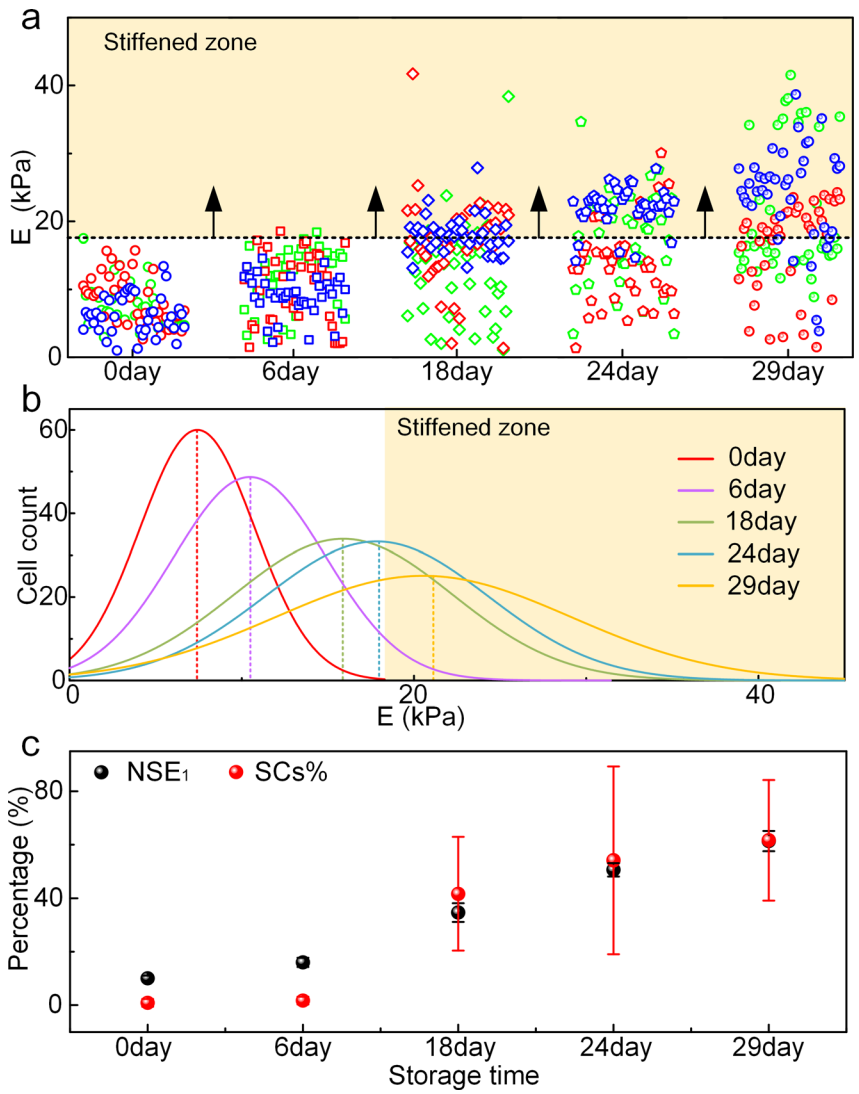

FIG. 4. Stiffness shifting of RBCs over storage time. (a) Young's modulus of the RBC sample, and the dot color represents the experimental group. The colored zone represents the stiffened zone where the modulus of RBCs is higher or equal to the maximum of 0 day RBCs' modulus. (b) Normal distribution of RBC Young's modulus, and the color represents the RBC type with different storage times. (c) The relationship between NSE_1 and SC% along storage time. Especially, $NSE_1 = SE_1 - SE_0$, and "SC%" means the percentage of stiffened cells.

stiffened zone, shown as the colored zone in Fig. 4(a), and the RBCs entranced the stiffened zone which are the stiffened cells (SCs). It is obvious that the number of SCs grows along the storage time. However, not every RBC showed obvious loss of deformability during storage, and some RBCs still maintained their low stiffness and did not entrance the stiffened zone. Especially for the 6 day RBCs, only a few RBCs become stiffened, which verified the margination behaviors of 6 day RBCs in Fig. 3(f). Because of the similar modulus distribution, the SE of 0 day and 6 day RBCs is close, and it could not distinguish 0 day RBCs and 6 day RBCs by their SE.

The normal distribution curve of the cell modulus is presented in Fig. 4(b). It is found that, as the storage time was elongated from 0 day to 29 days, the average modulus increases, and the modulus distributions move to the higher region and become more disperse. This result indicates that the RBCs with different storage times have a distinct modulus distribution, and the older RBCs have much higher stiffness. Allowing for the margination performance of aged RBCs in the microchannel in Fig. 3(f), the normalized separation efficiency (NSE) of RBCs

($NSE_1 = SE_1 - SE_0$, "1" means the position of 1 cm of the channel and "0" means 0 cm) was then calculated and is plotted with SC% in Fig. 4(c). SC% means the percentage of SCs in each RBC sample with different storage times. As shown in the black symbols, eliminating the impact of entrance on the SE, NSE is also increased over the storage time. As shown in the red symbols, the percentage of stiffed cells is increased by the storage time. Specifically, the variation of NSE and SC% along storage time are consistent, that is, the increasing trends of separation efficiency and cell modulus along the storage time are consistent, especially the results of 18 day, 24 day, and 29 day RBCs, and the percent reached the same level. On the other hand, as the storage time increased, more RBCs become stiff, and once they reached the stiffened zone, they could be separated from the normal RBCs by the margination technology. That is, the stiffening rate of RBCs by storage time could regulate the margination of aged RBCs in the microchannel.

IV. CONCLUSIONS AND DISCUSSION

In this study, we observed the approaching process of the particle to the channel wall during its margination and the disappearance of the center equilibrium position of particles flowing with the RBC suspension. Therefore, as a viscoelastic fluid, the RBC solution has its priority to realize the separation of aged RBCs from blood based on the deformability dependent margination, and the separation efficiency can be further enhanced substantially by the triangle cross-sectioned microchannel. Allowing for the visible distinction of separation efficiency between RBCs with different storage times obtained in the triangular microchannel, the recognition of storage time from the separation efficiency of aged RBCs could be realized. Then, the modulus of RBCs was investigated to clarify the mechanism between separation efficiency and storage time. It is found that a significant increase in the stiffness of RBCs happened after 18 days' storage time, while 6 days is not enough for RBCs to become stiff. Because of the disperse distribution on the Young's modulus, aged RBCs could not be all separated, and only those with modulus higher than the normal RBCs can be separated. More importantly, we demonstrated that the probability of aged RBCs' margination happening in the triangular channel, characterized by the SE of aged RBCs from normal RBCs, would increase along the storage time. The increasing variation is consistent with the stiffening rate of RBCs by different storage times, which is characterized by the increase in modulus. The regulating role of storage time on the margination of aged RBCs is confirmed.

As a deformability-based cell separation method, margination has been used to study cell sorting technology for decades. Tomaiuolo[19] reported biomechanical changes of RBCs in health and disease based on microfluidics, which offered some instructions of RBC deformability in margination-based RBC separation. Gordon *et al.*[35] reported that the electrical property changes of the cell enable effective discrimination through dielectrophoresis, which offered a sensitive method to detect the bovine red blood cell starvation age. Gagnon *et al.*[36] reported a buffer electric relaxation time tuning technique to discriminated bovine red blood cell starvation age based on dielectrophoresis, which offered a new sensitive method to detect the changes of the cell membrane and cytoplasm conductivity changes. Zhou *et al.*[37] reported the sensitivity of capillary loading of blood suspensions on the RBC deformability, which suggested some designs for the diagnosis of sepsis by microfluidics. Our work in this paper verified the overall deformability revolution of RBCs along storage time as reported before[35,36] and quantitatively investigated the relationship between aged RBCs' sorting and storage times. The modulus test indicated the sensitivity of each RBC to storage time and revealed the aging mechanism of RBCs during stored. On the other hand, the quantitative relationship between sorting efficiency and RBC storage time could be used to recognize the storage time of blood. The advantage of our work is to put up with a rapid simple and low cost means for separating aged RBCs with high efficiency and further detecting the quality of RBC products from a small fraction of the RBC sample, as well as could be used to discriminate between specific aged blood abnormalities. More importantly, the separation, analysis, and detection could be finished on one microfluidic device without impairment on RBCs. The mechanism could also be applied to the

separation of aged RBCs to decrease the blood transfusion risks and on the future commercialization of deformability-based cell sorting technology with high efficiency. However, the storage time used in this paper is not consecutive day by day, and the minimum interval of storage time that could be distinguished by the sorting efficiency is still unclear. Therefore, there is still a lot of work to confirm more accurate relationship between sorting efficiency and storage time for the detection of stored blood. The RBC solution not only provides viscoelasticity for aged RBCs to perform margination but also enhances the sorting efficiency by the collisions between RBCs. However, not every aged RBC could be separated from normal RBCs, and the sorting efficiency still cannot reach 100% because there are always some RBCs that maintain their deformability even when the storage time is elongated to 29 days. On the other hand, as the supporter of cell sorting, the application of RBC solution on blood detection is not convenient and safe, while the utilization of the viscoelastic polymer will lower the sorting efficiency. Therefore, it is necessary to find the perfect substitute of RBCs for cell sorting in blood detection.

ACKNOWLEDGMENTS

This work was supported by the NSFC (Nos. 51322501 and 51420105006) and the BJNSF (No. 3172018). The authors would also like to thank Bing Dong and Lei Yu for the support on the experiment.

[1]G.-S. Ted, "Structure and function of red and white blood cells," Medicine **37**(3), 119–124 (2009).
[2]J. Rey, P. A. Buffet, L. Ciceron, G. Milon, O. Mercereaupuijalon, and I. Safeukui, "Reduced erythrocyte deformability associated with hypoargininemia during Plasmodium falciparum malaria," Sci. Rep. **4**, 3767 (2014).
[3]M. C. Cheung, J. D. Goldberg, and Y. W. Kan, "Prenatal diagnosis of sickle cell anaemia and thalassaemia by analysis of fetal cells in maternal blood," Nat. Genet. **14**, 264–268 (1996).
[4]C. D. Brown, H. S. Ghali, Z. H. Zhao, L. L. Thomas, and E. A. Friedman, "Association of reduced red blood cell deformability and diabetic nephropathy," Kidney Int. **67**, 295–300 (2005).
[5]O. K. Baskurt, D. Gelmont, and H. J. Meiselman, "Red blood cell deformability in sepsis," Am. J. Respir. Crit. Care Med. **157**(2), 421–427 (1998).
[6]A. Kasukurti, C. D. Eggleton, S. A. Desai, and D. W. Marr, "FACS-style detection for real-time cell viscoelastic cytometry," RSC Adv. **5**(128), 105636 (2015).
[7]A. Kasukurti, C. D. Eggleton, S. A. Desai, and D. W. Marr, "The dynamic behavior of chemically "stiffened" red blood cells in microchannel flows," Microvasc. Res. **80**(1), 37 (2010).
[8]I. Safeukui, P. A. Buffet, G. Deplaine, S. Perrot, V. Brousse, A. Ndour *et al.*, "Quantitative assessment of sensing and sequestration of spherocytic erythrocytes by the human spleen," Blood **120**(2), 424–430 (2012).
[9]R. E. Waugh, M. Narla, C. W. Jackson, T. J. Mueller, T. Suzuki, and G. L. Dale, "Rheologic properties of senescent erythrocytes: Loss of surface area and volume with red blood cell age," Blood **79**(5), 1351–1358 (1992).
[10]H. Relevy, A. Koshkaryev, N. Manny, S. Yedgar, and G. Barshtein, "Blood banking-induced alteration of red blood cell flow properties," Transfusion **48**(1), 136 (2008).
[11]A. R. Haradin, R. I. Weed, and C. F. Reed, "Changes in physical properties of stored erythrocytes relationship to survival in vivo," Transfusion **9**(5), 229–237 (1969).
[12]T. Takei, N. A. Amin, G. Schmid, N. Dhingra-Kumar, and D. Rugg, "Progress in global blood safety for HIV," J. Acquired Immune Defic. Syndr. **52**(2), S127 (2009).
[13]J. C. Zimring, "Established and theoretical factors to consider in assessing the red cell storage lesion," Blood **125**(14), 2185–2190 (2015).
[14]S. A. Glynn, H. G. Klein, and P. M. Ness, "The red blood cell storage lesion: The end of the beginning," Transfusion **56**(6), 1462 (2016).
[15]A. D'Alessandro, A. G. Kriebardis, S. Rinalducci, M. H. Antonelou, K. C. Hansen, I. S. Papassideri *et al.*, "An update on red blood cell storage lesions, as gleaned through biochemistry and Omics technologies," Transfusion **55**(1), 205–219 (2015).
[16]S. M. Frank, B. Abazyan, M. Ono *et al.*, "Decreased erythrocyte deformability after transfusion and the effects of erythrocyte storage duration," Anesth. Analg. **116**(5), 975–981 (2013).
[17]M. Abkarian, M. Faivre, R. Horton *et al.*, "Cellular-scale hydrodynamics," Biomed. Mater. **3**(3), 034011 (2008).
[18]G. Tomaiuolo, L. Lanotte, R. D'Apolito *et al.*, "Microconfined flow behavior of red blood cells," Med. Eng. Phys. **38**(1), 11 (2016).
[19]G. Tomaiuolo, "Biomechanical properties of red blood cells in health and disease towards microfluidics," Biomicrofluidics **8**(5), 051501 (2014).
[20]H. Zhao, E. S. G. Shaqfeh, and V. Narsimhan, "Shear-induced particle migration and margination in a cellular suspension," Phys. Fluids **24**(1), 011902 (2012).
[21]K. Vahidkhah and P. Bagchi, "Microparticle shape effects on margination, near-wall dynamics and adhesion in a three-dimensional simulation of red blood cell suspension," Soft Matter **11**(11), 2097–2109 (2015).
[22]R. D'Apolito, G. Tomaiuolo, F. Taraballi *et al.*, "Red blood cells affect the margination of microparticles in synthetic microcapillaries and intravital microcirculation as a function of their size and shape," J. Controlled Release **217**(8 Supplement), 263–272 (2015).

[23]R. D'Apolito, F. Taraballi, S. Minardi *et al*., "Microfluidic interactions between red blood cells and drug carriers by image analysis techniques," Med. Eng. Phys. **38**(1), 17 (2016).
[24]H. W. Hou, A. A. Bhagat, A. G. Chong, P. Mao, K. S. Tan, J. Han *et al*., "Deformability based cell margination–a simple microfluidic design for malaria-infected erythrocyte separation," Lab Chip **10**, 2605–2613 (2010).
[25]H. W. Hou, L. Wu, D. P. Amador-Munoz, M. P. Vera, A. Coronata, J. A. Englert *et al*., "Broad spectrum immunomodulation using biomimetic blood cell margination for sepsis therapy," Lab Chip **16**(4), 688–699 (2016).
[26]S. Huang, H. W. Hou, T. Kanias, J. T. Sertorio, H. Chen, D. Sinchar *et al*., "Towards microfluidic-based depletion of stiff and fragile human red cells that accumulate during blood storage," Lab Chip **15**(2), 448 (2015).
[27]J. C. Mcdonald, D. C. Duffy, J. R. Anderson, D. T. Chiu, H. Wu, O. J. Schueller *et al*., "Fabrication of microfluidic systems in poly (dimethylsiloxane)," Electrophoresis **21**, 27–40 (2000).
[28]C. Liu, C. Xue, X. Chen *et al*., "Size-based separation of particles and cells utilizing viscoelastic effects in straight microchannels," Anal. Chem. **87**(12), 6041–6048 (2015).
[29]G. D'Avino *et al*., "Single line particle focusing induced by viscoelasticity of the suspending liquid: Theory, experiments and simulations to design a micropipe flow-focuser," Lab Chip **12**(9), 1638–1645 (2012).
[30]A. M. Ruiz-Zapata, M. H. Kerkhof, B. Zandieh-Doulabi, S. Ghazanfari, T. H. Smit, and M. N. Helder, "Influences of extracellular matrices on myofibroblast differentiation in pelvic organ prolapse," in TERMIS-EU (2016).
[31]H. Hertz, "On the elastic contact of elastic solids," J. Reine Angew. Math. **92**, 156–171 (1881).
[32]S. Shin, J. Nam, and H. Lim, "Continuous separation of microparticles in a microfluidic channel via the elasto-inertial effect of non-Newtonian fluid," Lab Chip **12**(7), 1347 (2012).
[33]M. A. Tehrani, "An experimental study of particle migration in pipe flow of viscoelastic fluids," J. Rheol. **40**, 1057–1077 (1996).
[34]Y. Chen, D. Li, Y. Li, J. Wan, J. Li, and H. Chen, "Margination of stiffened red blood cells regulated by vessel geometry," Sci. Rep. **7**(1), 15253 (2017).
[35]J. E. Gordon, Z. Gagnon, and H. C. Chang, "Dielectrophoretic discrimination of bovine red blood cell starvation age by buffer selection and membrane cross-linking," Biomicrofluidics **1**(4), 044102 (2007).
[36]Z. Gagnon, J. Gordon, S. Sengupta *et al*., "Bovine red blood cell starvation age discrimination through a glutaraldehyde-amplified dielectrophoretic approach with buffer selection and membrane cross-linking," Electrophoresis **29**(11), 2272 (2008).
[37]R. Zhou, J. Gordon, A. F. Palmer *et al*., "Role of erythrocyte deformability during capillary wetting," Biotechnol. Bioeng. **93**(2), 201–211 (2006).